About the Atypical Behavior of CrO_3, MoO_3, and WO_3 during Their UV Laser Ablation/Ionization

Frédéric Aubriet*,† and Jean-François Muller*,‡

Laboratoire de Spectrométrie de Masse et de Chimie Laser, IPEM−Université de Metz−1, boulevard Arago, 57078 Metz Cedex 03, France

Received: February 14, 2002; In Final Form: April 25, 2002

Pulsed-tripled Nd:YAG and excimer laser ablation of chromium, molybdenum, and tungsten trioxide at high power density has been found to generate significant yields of oxygenated cluster ions. They were analyzed by Fourier transform ion cyclotron resonance mass spectrometry. Two kinds of cluster ions were considered. The first ones are largely oxygen-deficient and their formation are the result of aggregation processes between neutrals and ions according to results obtained in the study of other transition-metal oxides. The second ones are $M_nO_{3n}^+$ stoichiometric and $M_nO_{3n-2}^+$ and $M_nO_{3n-1}^+$ slightly substoichiometric species (with M = Cr, Mo, and W and $n = 1-6$). The production of these latter ions decreases dramatically with the power density deposited on the sample surface. This behavior is non-wavelength-dependent. Previously, Knudsen effusion mass spectrometry studies and thermodynamic considerations allowed us to determine their formation pathways. These ions come from interaction between electrons and neutral species generated by vaporization or sublimation of the sample near the laser impact or both. Electrons are emitted according to various processes during laser/matter interaction conditions.

Introduction

The study of ion formation processes after laser irradiation of inorganic compounds is very critical. As a consequence, no general model, as far as we know, has been postulated up to now. Nevertheless, several papers dealing with this fundamental issue have been published, and different models have been proposed.[1−7] Amuroso et al. recently reviewed the studies aimed at understanding the laser ablation process and its basic microscopic mechanism, especially for metallic and inorganic compounds.[8]

At the beginning of the 1980s, Marien and DePauw[9] considered that two mechanisms could explain the cluster-ion emission in laser ablation mass spectrometry (LA-MS): recombination and unimolecular dissociation before detection. The recombination model assumes that, after laser ablation, particles (neutrals, ions, atoms, and aggregates) recombine in the gas phase. The factors that govern each of the processes are distinct. According to these authors, the ejection of a lattice fragment occurs if the involved energy is low enough to avoid complete atomization. In this case, some of the weakest bonds in the crystal have to be preferentially broken. In the recombination model, particles properly correlated in time, space, and velocity recombine in the gas phase to give the most stable species. Finally, these authors considered that both pathways of ion formation occur simultaneously in LA-MS experiments. These considerations have been recently supported by the study of $Co(NO_3)_2 \cdot 6H_2O$.[10] Liu et al. highlighted two pathways of cluster ion formation. The first one accounts for the $Co_nO_m^+$ ion production, and it is consistent with recombination processes, whereas $\{Co[Co(NO_3)_2]_x(H_2O)_y\}^+$ ions are directly ejected from the sample surface under photon bombardment.

Dennemont and Landry,[11] Lafargue et al.,[12] Gibson,[13] Hachimi et al.,[14,15] and Liu et al.[16] are among authors who think that cluster ions are formed via the growth of smaller entities and sequential addition of neutral molecules to precursor ions. Some other studies seem to confirm this conclusion: Chaoui et al.[17] obtained, in particular, similar time-of-flight laser-microprobe mass spectrometry (TOF-LMMS) fingerprints when $PbTiO_3$ and a PbO/TiO_2 equimolar mixture were successively studied. In addition, it has been demonstrated that dissociative processes may follow the aggregation by excess of internal energy or by collision with neutrals in the laser plume or both.[18] Finally, Maunit et al.[19] proposed an alternative formation mechanism to explain the observation of highly oxygen-deficient species in the iron oxide laser ablation. These authors showed that the dimer Fe_2^+ was produced by a reactive process between Fe^+ ion and FeO neutral with the simultaneous loss of oxygen.

In summary, it appears that the formation of positive cluster ions generated by laser ablation is the sum of several processes, depending (i) on the nature of the metal (in particular the electronic d shell filling[20]), (ii) on the metal/oxygen ratio in the studied oxide, (iii) on instrumental parameters (wavelength, pulse duration, power density, ...), and (iv) on the presence of other species present in the studied compounds.[18,21,22] Therefore, the absence of a laser ablation model for inorganic compounds is not surprising, regarding the complexity of the involved processes. All previous studies only reported the detection of positive ions for which the metal valence was lower or equal to the higher valence of the metal in the solid phase.[21]

The study of nearly 60 mineral compounds (oxides and salts) by laser ablation Fourier transform ion cyclotron resonance mass spectrometry (LA-FTICRMS) at the wavelength of 355 nm under power density between 3×10^{10} and 5×10^6 W/cm^2 [20] allowed us to detect a full range of cluster ions, especially in the study of transition-metal oxides. Their formation is generally well-described by the processes previously reported,[12−18] except in some particular cases. Hexavalent chromium, molybdenum,

* To whom correspondence should be addressed.
† E-mail: aubriet@lsmcl.sciences.univ-metz.fr. Phone: (33) 3 87 31 58 53. Fax: (33) 3 87 31 58 51.
‡ E-mail: jfmuller@lsmcl.sciences.univ-metz.fr. Phone: (33) 3 87 31 58 57. Fax: (33) 3 87 31 58 51.

10.1021/jp020432r CCC: $22.00
Published on Web 06/01/2002

and tungsten oxides, however, have an atypical behavior: heptavalent metal valence sites were, in particular, highlighted in some positive cluster ions. That is the reason that the investigation of the mechanisms involved in the laser ablation of CrO_3, MoO_3, and WO_3 was undertaken. Experiments in various instrumental conditions of power density and wavelength have been performed. The results were compared to previous ones obtained using desorption laser vaporization (DLV)[14,23−27] or Knudsen effusion cell coupled with mass spectrometry (KEMS).[28−35]

Experimental Section

Chemicals. All commercial chemicals were of analytical reagent grade. Chromium(VI) oxide (99%) and tungsten(VI) oxide (99.995%) were purchased from Aldrich (Milwaukee, WI) and molybdenum(VI) oxide (99%) from Merck (Germany).

Instrumentation. The analyses were performed using a laser microprobe FTICR mass spectrometer that has been described in detail elsewhere.[36,37] This instrument is a modified differentially pumped, dual-cell Nicolet Instrument FTMS 2000 (Finnigan FT/MS, now named ThermoFinnigan, Madison, WI) operated with a 3.04 T magnetic field and coupled to a reflection laser interface. The viewing system, using an inverted Cassegrain optics design, allows us to visualize the sample with 300-fold magnification. A sample probe fitted with motorized micromanipulators into the three spatial directions permits us to attain a spatial accuracy of less than 10 μm. The ionization step was performed using the third harmonic of a Q-switch Nd:YAG laser ($\lambda = 355$ nm, pulse duration 4.3 ns, output energy used 0.8 mJ). Alternatively, an excimer laser charged with an ArF mixture ($\lambda = 193$ nm, pulse duration 23 ns, output energy used 1.6 mJ) was used. The diameter of the laser beam on the sample (placed inside the source cell) can be adjusted by means of the internal lens and an external adjustable telescope from 5 to several hundred micrometers, which corresponds to a power density ranging from 10^{10} to 10^6 W/cm^2. The experiment sequence used for these analyses is as described: Ions are formed by laser ablation in the source cell (residual pressure 10^{-5} Pa). During the ionization event, the conductance limit plate between the two cells and the source trap plate are kept at a trapping potential of typically 2 V (−2 V in negative detection mode) or at a lower potential in some particular cases (down to 0.25 V). A variable delay period follows, during which ion/molecule reactions can occur. Ions are then excited by a frequency excitation chirp, and the resulting image current is detected, amplified, digitized, apodized (Blackman-Harris, three-terms), and Fourier-transformed to produce a mass spectrum.

Some experiments were performed in positive detection mode with Cr^+, Mo^+, or W^+ ejection[38] to enhance the detection of the signal delivered by mixed oxygenated cluster ions. Ejection of a large concentration of a single type of ion from the ICR cell often enhances the signal because of reduced Coulomb ejection of other ions. Moreover, these M^+ ions may also be involved in dissociation of large cluster ions, even if it may be considered that the likelihood of ion/cluster collision rate was low. Each FTICR mass spectrum resulted from the average of 100 laser shots fired on different spots. The ion assignment was performed by the measurement of exact mass after calibration and the identification of the isotopic distribution. For example, Figure 1 reports the comparison of the (a) theoretical and (b) experimental isotopic distribution and the exact mass measurement for $Mo_2O_4^+$ ion.

Power density measurements were performed by measuring, first, the laser spot diameter at the sample surface and, second, the output laser energy. An attenuation factor allowed us to consider the absorption of optics in the FTICR microprobe instrument. The measurement reliability, in the used power density range, was better than 10%.

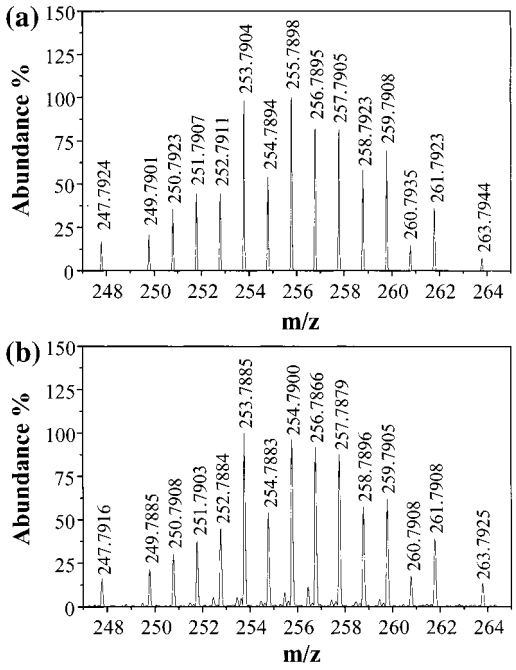

Figure 1. Theoretical (a) and experimental (b) isotopic distribution of the $Mo_2O_4^+$ ion.

Results

Mass spectra obtained by direct laser ablation of chromium, molybdenum, and tungsten trioxide (respectively, CrO_3, MoO_3, and WO_3) using the 355 nm output of a Nd:YAG laser at a power density of 3.6×10^{10} W/cm^2 are shown in Figure 2. A large quantity of $M_xO_y^+$ ions is produced. The analysis of the LA-FTICR mass spectra obtained in these conditions of laser power density reveals a common behavior for all of the studied compounds. In particular, large cluster ions, including up to six metal atoms for CrO_3 and MoO_3 oxides and four metal atoms for WO_3, are detected. The detected ions for these three compounds have the same composition and may be gathered in the following series: MO_{0-3}^+; $M_2O_{2-6}^+$; $M_3O_{4-9}^+$; $M_4O_{6-12}^+$; $M_5O_{11-15}^+$. However, it is interesting to note that laser ablation of the chromium trioxide compound does not lead to the detection of the highest oxygenated species, whatever the considered ion series. Furthermore, the ions including more than four molybdenum or chromium atoms have a poor abundance, as compared to the MO_{0-3}^+; $M_2O_{2-6}^+$; $M_3O_{4-9}^+$ and $M_4O_{6-12}^+$ series. This observation suggests that the dramatic drop in $M_xO_y^+$ ion intensities between $x = 4$ and $x = 5$ is thermodynamically significant. Structural considerations may certainly be involved. In contrast to the study of other inorganic compounds by LA-MS,[18] no Poisson distribution is observed. This suggests that the cluster ion formation pathways, in the study of these compounds, are atypical. As a consequence, aggregative mechanisms may not only be taken into account to explain the ion formation processes. The obtained results are in good agreement with Cassady et al.[24] when molybdenum dioxide and trioxide are characterized by DLV mass spectrometry at 532 nm with an energy per pulse between 1 and 10 mJ and with a pulse duration of 10 ns. However, the highly oxygenated species for each $Mo_{0-4}O_y^+$ ion series are not

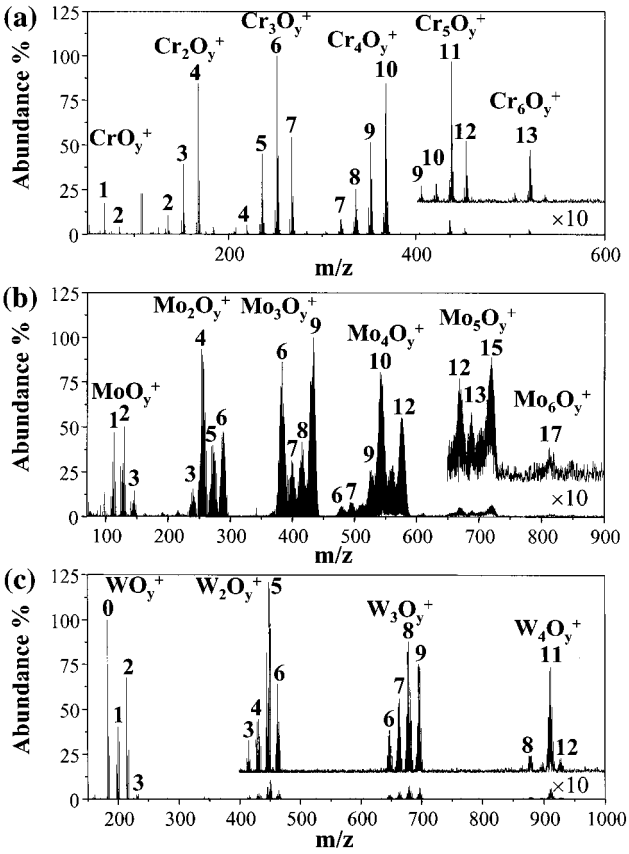

Figure 2. The positive ion laser ablation mass spectra of (a) chromium, (b) molybdenum, and (c) tungsten trioxides with a wavelength of 355 nm and a power density of 3.6×10^{10} W/cm^2.

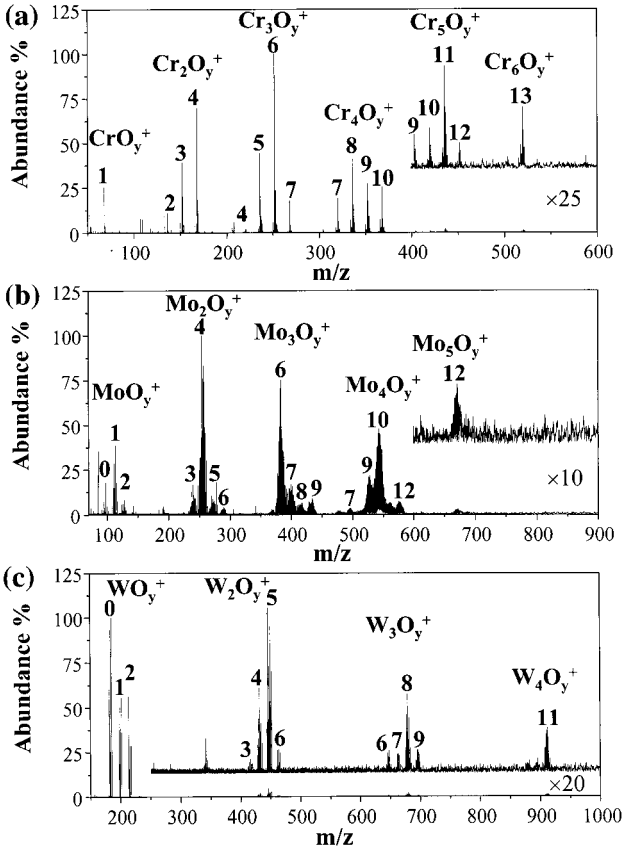

Figure 3. The positive ion laser ablation mass spectra of (a) chromium, (b) molybdenum, and (c) tungsten trioxides with a wavelength of 355 nm and a power density of $\sim 2 \times 10^9$ W/cm^2.

observed, except when experiments are carried out with a pulsed CO_2 laser (10.6 μm) on the MoO_2 compound at high power density. In that case, the total energy applied to the sample is approximately an order of magnitude higher than for Nd:YAG (532 nm).[24]

When the power density is decreased down to $\sim 2 \times 10^9$ W/cm^2 (Figure 3), the fingerprint of the three considered trioxides is significantly modified. The abundance of the highly oxygenated species $Mo_nO_{3n}^+$ and $Mo_nO_{3n-1}^+$ decreases. At this power density and under these experimental conditions, the distribution of the observed cluster ions for molybdenum and tungsten trioxide in positive mode is very similar to previous LA-FTICRMS results.[24−27] No data were available for the CrO_3 compound to allow for comparison, even though some authors[14,27] investigated this compound by LA-FTICRMS in positive ion detection mode. They only reported the formation of Cr^+ ion. The obtained behavior for highly oxygenated species was previously observed by Cassady et al.[24] when molybdenum dioxide was examined at the wavelength of 10.6 μm. These species were observed at high laser power density, but they disappeared when laser power density was lowered.

KEMS studies reveal that large amounts of $(MoO_3)_{1-3}$ neutral species are formed when the MoO_2 compound is heated at 1500 K.[31] Therefore, these molybdenum species may also be abundant neutrals in the plume produced by laser ablation because of the high temperature reached during the laser/matter interaction. In addition, Cassady et al. correlated the detection of these highly oxygenated species with the intense absorption bands of molybdenum dioxide at 9.5−12 μm, more particularly, with the symmetric Mo−O stretch around 10.5−10.6 μm. These authors concluded that the production of these ions is wavelength-dependent.[24] This conclusion is in disagreement with our results. We also observe a significant production of $(MoO_3)_n^+$ ions at 355 nm, which indicates the independence of the production of these ions on the wavelength. To confirm this conclusion, experiments were performed with another wavelength, the 193 nm radiation of an ArF excimer laser. The three trioxide compounds were studied, but we report only the MoO_3 results in this paper.

The ablation behavior of the molybdenum trioxide at the wavelength of 193 nm is comparable to the results obtained at 355 nm (see in Figure 4). When high power density, 5×10^9 W/cm^2, is used (Figure 4a), the observed ions and their relative distribution are comparable to those obtained at 355 nm with a power density of 3.6×10^{10} W/cm^2. The abundance of the highly oxygenated species decreases dramatically when the power density is lowered to $\sim 1.4 \times 10^8$ W/cm^2 (Figure 4b). However, a dramatic decrease of large cluster ion intensity is also observed at 193 nm, whatever the used power density. The $M_2O_{2-6}^+$, $M_3O_{4-9}^+$, and $M_4O_{6-12}^+$ ions are produced in poor abundance. This behavior may be related to two experimental parameters, first, the energy of each photon at 193 nm and, second, the pulse duration (see Experimental Section). It was previously observed in the study of alkaline chromate,[22] that both the increase of energy per photon and the increase of laser pulse duration induce an internal energy increase for ions, which leads to an increase of fragmentation by dissociative processes. The same explanation may be given to explain the obtained results.

Consequently, the development of the fingerprint for CrO_3, MoO_3, and WO_3 is non-wavelength-dependent. The laser power density deposited at the sample surface is a more critical parameter, which greatly influences the nature and the relative distribution of the $M_xO_y^+$ ions.

TABLE 1: Positive Ions Observed in Knudsen Effusion Mass Spectrometry Study of Chromium, Molybdenum, and Tungsten Trioxide

	CrO_3		MoO_3		WO_3
cluster ions	McDonald and Margrave[a]	Washburn[b]	Berkowitz et al.[c]	Fialko et al.[d]	Ackermann and Rauh[e]
MO^+			detected	detected	detected
MO_2^+				detected	detected
MO_3^+				detected	detected
$M_2O_3^+$	detected	detected			
$M_2O_4^+$	detected	detected		detected	
$M_2O_5^+$	detected	detected		detected	detected
$(MO_3)_2^+$		detected	detected	detected	detected
$M_3O_4^+$		detected			
$M_3O_5^+$		detected			
$M_3O_6^+$	detected	detected			
$M_3O_7^+$	detected	detected			
$M_3O_8^+$		detected		detected	detected
$(MO_3)_3^+$	detected	detected	detected	detected	detected
$M_4O_7^+$		detected			
$M_4O_8^+$	detected	detected			
$M_4O_9^+$	detected	detected			
$M_4O_{10}^+$	detected	detected			
$M_4O_{11}^+$		detected		detected	detected
$(MO_3)_4^+$	detected	detected	detected	detected	detected
$M_5O_{13}^+$	detected	detected			
$M_5O_{14}^+$		detected			
$(MO_3)_5^+$	detected	detected	detected	detected	detected
$(MO_3)_6^+$		detected			

[a] According to ref 28. [b] According to ref 29. [c] According to ref 32. [d] According to ref 33. [e] According to ref 35.

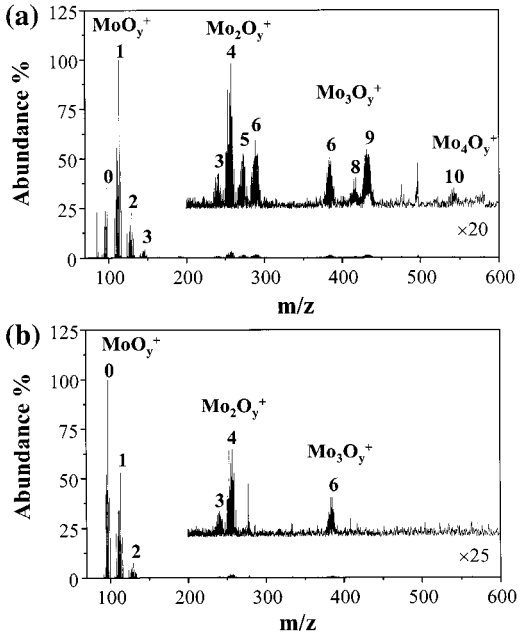

Figure 4. The positive ion laser ablation mass spectra of molybdenum trioxide with a wavelength of 193 nm and a power density of (a) 5×10^9 and (b) $\sim 1.4 \times 10^8$ W/cm^2.

Discussion

The non-wavelength dependence of chromium, molybdenum, and tungsten trioxide behavior, in contrast to experiments performed with other inorganic compounds,[22] leads us to consider that aggregative processes may not be alone involved in the formation of cluster ions, especially the highly oxygenated ones. In addition, the high power density required to observe these ions is unusual in the study of inorganic compounds.[20]

To better understand the formation of the $M_xO_y^+$ ions, our results were compared with other mass spectrometric techniques, especially static secondary ion mass spectrometry (s-SIMS) and KEMS. The investigation of CrO_3[39] and MoO_3[39−41] by s-SIMS leads to the detection of few ions. M^+ and MO^+ (with M = Cr and Mo) and $CrOH^+$ and MoO_2^+ are, in particular, observed.

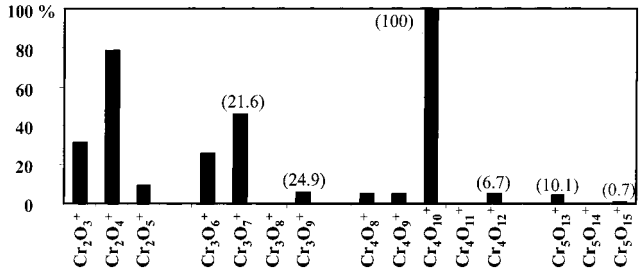

Figure 5. Knudsen effusion mass spectra of chromium trioxide by using experimental data from ref 28 obtained at 519 K with electron energy of 50 eV. In parentheses, the ion intensities obtained by Washburn[29] at 17 eV with an effusion temperature of 498 K are given.

Unfortunately, to our knowledge, no experiments have been performed on the WO_3 compound.

KEMS studies of CrO_3,[28−30] MoO_3,[31−33] and WO_3[34,35] are more numerous and more interesting. In most of these studies, the used experimental conditions lead to the production of significant amounts of $M_xO_y^+$ ions. The main detected species ($M_nO_{3n-2}^+$, $M_nO_{3n-1}^+$, and $M_nO_{3n}^+$) have generally a stoichiometry close to the studied compounds and are generated, according to Washburn,[29] by direct ionization of the corresponding neutrals under electron ionization conditions. It is also suggested that largely substoichiometric $Cr_xO_y^+$ ions may be produced by neutral dissociative processes. Table 1 summarizes the detected ions in KEMS studies of CrO_3, MoO_3, and WO_3 compounds. The distribution of these species are reproduced on Figure 5 for CrO_3, according to the results of McDonald et al.[28] MoO_3 results were previously reported by Fialko et al.[33]

For molybdenum trioxide, the obtained mass spectrum at 355 nm with a power density of 3.6×10^{10} W/cm^2 can be considered as a superposition of the MoO_3 mass spectra obtained by KEMS[33] and by DLV-FTICRMS at 532[24] or at 355 nm with a power density of $\sim 2.2 \times 10^9$ W/cm^2 (Figure 3b).

For this reason, it may be assumed that several processes of ion formation take place when CrO_3, MoO_3, and WO_3 are laser ablated under high power density conditions. The first one leads to the formation of largely substoichiometric ions by recombination in the gas phase, as is observed in the study of other

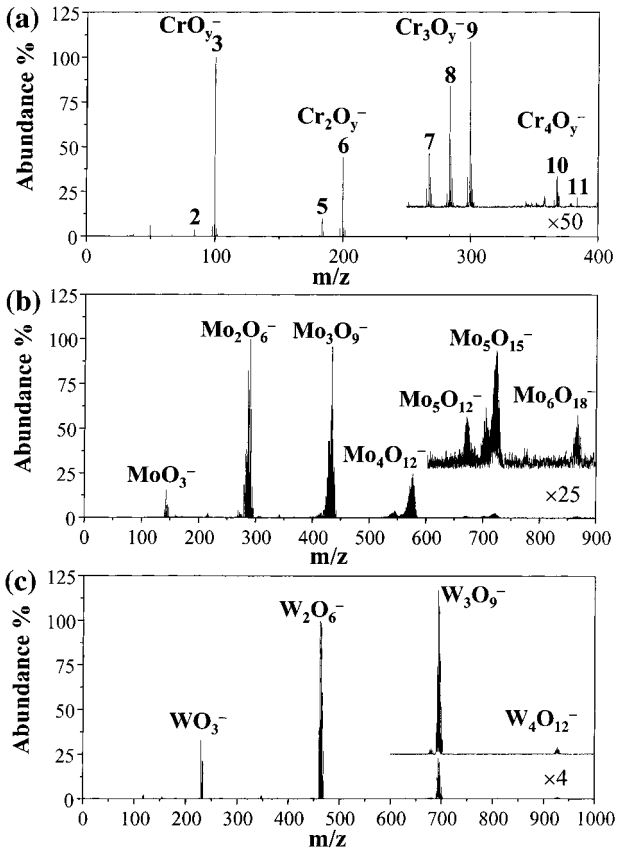

Figure 6. The negative ion laser ablation mass spectra of (a) chromium, (b) molybdenum, and (c) tungsten trioxides with a wavelength of 355 nm and a power density of 3.6×10^{10} W/cm^2.

transition-metal oxides.[20] The second one is specific to high laser power density ($>10^{10}$ W/cm^2) and leads to the production of stoichiometric $M_nO_{3n}^+$ or slightly substoichiometric $M_nO_{3n-2}^+$ and $M_nO_{3n-1}^+$ species. The detection of the latter in KEMS experiments seems to indicate that their formation mechanisms are close to those observed in KEMS experiments (i.e., production of large neutral species by sublimation or vaporization and ionization by electron ionization).

The laser/matter interaction at high power density is characterized by a high temperature at the laser impact and by a high electronic density. These two parameters have a significant influence on the behavior of chromium, molybdenum, and tungsten trioxide at 3.6×10^{10} W/cm^2. The KEMS of these three compounds show that large amounts of M_nO_{3n}, M_nO_{3n-1}, and M_nO_{3n-2} are produced when they are heated between 400 and 1600 K. The temperature reached in the laser impact region suggests that large amounts of M_nO_{3n-x} ($x = 0-2$) neutral species may be formed during and after (i.e., as long as the temperature of the sample is sufficiently high) the laser/matter interaction. The negative ion analysis of chromium, molybdenum, and tungsten trioxide at the wavelength of 355 nm with a power density of 3.6×10^{10} W/cm^2, reported in Figure 6, leads to the detection of $(MO_3)_n^-$ ions (M = Cr, Mo, or W and $n = 1-6$). Only small amounts of $M_nO_{3n-1}^-$ and $M_nO_{3n-2}^-$ are detected in the study of chromium trioxide. The non-wavelength dependence of the CrO_3, MoO_3, and WO_3 behavior in the negative ion detection mode[42] and the high electron affinity of $(MO_3)_n$ neutrals, gathered in Table 2, suggest that the negative ion mass spectra of these three compounds are indicative of neutral species formed during laser irradiation. This interpretation is supported by the results obtained by Maleknia et al. in the thermal desorption/electron capture negative ionization study

TABLE 2: Electron Affinities in eV of Some M_xO_y Species (M = Cr, Mo, and W)

	CrO_3	MoO_3	WO_3
MO_2	2.413 ± 0.008[a] 2.52[b]	2.01[b]	1.93[b]
MO_3	3.64 ± 0.18[c] 3.49[b]	2.85 ± 0.21[c]	3.94 ± 0.2[c]
$(MO_3)_2$	1.6 ± 0.3[d]		
$(MO_3)_3$	1.8[d]		

[a] According to ref 44. [b] B3LYP calculation results according to ref 43. [c] According to ref 45. [d] According to ref 30.

of MoO_3 and WO_3[46] and by the KEMS study of CrO_3 in negative detection mode performed by Ling-Fai Wang et al.[30] Both papers clearly indicate the formation of $(MO_3)_n^-$ anions by electron-capture processes and by dissociative electron attachment.[30] In this respect, the formation of CrO_2^-, CrO_3^-, MoO_2^-, and WO_2^- through electron-capture processes by the corresponding neutral molecules has been observed during their condensation in a solid neon matrix after reaction between O_2 and laser-ablated chromium, molybdenum, or tungsten atoms.[43] For all of these reasons, it is reasonable to assume that the high temperature reached during the laser ablation process at high power density may induce the formation of large amounts of M_nO_{3n}, M_nO_{3n-1}, and M_nO_{3n-2} species in the gas phase.

It is well-established from experimental[47] and theoretical[48] studies that two laser/matter regimes can be distinguished as a function of the laser power density. The process involved at low laser power density is usually called laser desorption and leads to the restricted sputtering of the sample surface. For example, the laser power density used in the well-known MALDI technique (matrix-assisted laser desorption/ionization) does not exceed 10^7 W/cm^2.[49] When a higher power density is used, laser irradiation leads to the ejection of larger amounts of matter. In these experimental conditions, the interaction of photons with an energy higher than the work function (i.e., energy required for an electron to escape from the surface) of the metal or of the inorganic compound leads to the formation of an electron swarm, which instantaneously leaves the surface according to the photoelectric effect.[50] In general, there are three different ways by which electrons can be expelled from a target: photon-induced electron emission (photoelectronic effect), photon emission due to a high temperature (thermoelectronic effect), and field emission. The photoelectronic effect results from the photon absorption by the surface of the target, especially metals. The energy of the impinging photon is used to emit an electron out of the target. The difference between the photon energy, $h\nu$, and the work function, W_a, of the target (i.e., the excess of energy) is transformed into kinetic energy according eq 1:

$$h\nu = W_a + {}^1/_2 m v^2 \qquad (1)$$

This equation shows that the kinetic energy of the electron generated by photoelectronic effect cannot be greater than the photon energy (6.42 eV at 193 nm and 3.49 eV at 355 nm). Furthermore, the electron work function, W_a, of the most common metals has values ranging from 3 to 5.5 eV.[51] These values suggest that, in our experimental conditions, the kinetic energy of photoelectrons does not exceed several electronvolts. Unfortunately, no data of W_a for the three considered trioxides have been found, and we were not able to evaluate the kinetic energy of the photoelectrons generated by the laser ablation of trioxide compounds. The increase of the power density on the target leads to saturation effects. Hence, the excess photons are

TABLE 3: Ionization Energy (IE) of Some $M_xO_y^0$ Neutral Species and Appearance Energy (AE) of Some $M_xO_y^+$ Cluster Ions in eV for Chromium, Molybdenum, and Tungsten

	chromium		molybdenum		tungsten	
	IE	AE	IE	AE	IE	AE
$MO_2^{0/+}$	9.7 ± 0.2^a		9.4 ± 0.6^e		9.9 ± 0.6^e	14.2^h $(WO_3)^d$
$(MO_3)^{0/+}$	11.6 ± 0.5^b		12.0 ± 0.6^e		11.7 ± 0.6^e	
$M_2O_5^{0/+}$		18.9^c $(CrO_3)_3^d$	10.0^f	14.5^f $(MoO_3)_2^d$		15.3 ± 0.2^g $(WO_3)_2^d$
$(MO_3)_2^{0/+}$			12.1 ± 0.6^f		12.2 ± 0.2^g	
$M_3O_8^{0/+}$		16.7^c $(CrO_3)_3^d$	12.2^f	14.5^f $(MoO_3)_3^d$		14.6 ± 0.2^g $(WO_3)_3^d$
$(MO_3)_3^{0/+}$	11.5^c		12.0 ± 1.0^f		12.0 ± 0.2^g	
$M_4O_{11}^{0/+}$		15.3^c $(CrO_3)_4^d$				13.9 ± 0.2^g $(WO_3)_4^d$
$(MO_3)_4^{0/+}$	11.1^c				12.0 ± 0.2^g	

[a] According to ref 55. [b] According to ref 56. [c] According to ref 29. [d] Neutral parent. [e] According to ref 34. [f] According to ref 31. [g] According to ref 57. [h] According to ref 58.

absorbed by the target and eventually lead to thermal emission of electron according to the Boltzmann factor, k_BT. The number of thermal-emitted electrons can be estimated with the Richardson−Dushman equation, eq 2:

$$j(T) = C_R T^2 \exp(-\Phi/k_BT) \quad (2)$$

where $j(T)$ is the current density of the emitted electrons, C_R is the Richardson constant, Φ is the thermal work function of the emitter, and k_B is the Boltzmann constant. The thermal emission process leads to electrons with a broad kinetic energy spread according to the Maxwell velocity distribution. Furthermore, thermal electrons are emitted during a longer period of time than photoelectrons, because their emission also occurs after the laser irradiation.[50a] Simulation of picosecond laser-induced electron emission from silicon indicated that thermionic electron emission yield becomes preponderant at high power density when low wavelengths are used.[52] It is generally reported that thermionic electron kinetic energy is close to the photoelectron one.[53] Consequently, the energy of thermal electrons does not exceed some electronvolts. Finally, electrons can be emitted from a target due to field emission. The work function of solid surfaces is strongly influenced by electrostatic and electromagnetic fields. Thus, by applying an electric field to the emitter, the work function can be lowered, leading to an increase of the probability for electron emission due to tunneling effects. For these reasons, the laser ablation of chromium, molybdenum, and tungsten trioxide, especially at high power density, may lead to the emission of significant amounts of electrons by various processes. Moreover, the emitted electrons may gain energy in the laser field through inverse bremsstrahlung (IB) absorption.[5,8,54] If the power density exceeds the plasma ignition threshold, observed around 5×10^8 W/cm^2 for each of the three studied compounds, additional energy coupling occurs due to breakdown of the plasma. The IB process involves the interaction of photons with free electrons, which gain energy from the laser beam during collisions with neutral and ionized atoms.[5,8] Finally, the kinetic energy of thermal electrons and photoelectrons is significantly increased.

In electron ionization, two mechanisms may be considered; the first one results from the simple ionization of the molecules according to eq 3:

$$AB + e^- \rightarrow AB^+ + 2e^- \quad (3)$$

The second one is consistent with a dissociative ionization mechanism according to the following eqs 4 and 5:

$$AB + e^- \rightarrow A^+ + B + 2e^- \quad (4)$$

$$AB + e^- \rightarrow A^+ + B^- + e^- \quad (5)$$

The first process (eq 3) is governed by the neutral parent ionization energy, whereas appearance energy and electron affinity govern the two latter mechanisms. Ionization energy of some M_xO_y species and appearance energy of some $M_xO_y^+$ ions for chromium, molybdenum, and tungsten are reported in Table 3. Washburn[29] demonstrated that both processes may occur simultaneously, in the KEMS study of the chromium trioxide. Stoichiometric $Cr_nO_{3n}^+$ or slightly substoichiometric $Cr_nO_{3n-2}^+$ and $Cr_nO_{3n-1}^+$ species with $n = 3-6$ are formed by direct ionization of the neutrals, whereas $Cr_2O_{3-5}^+$, $Cr_3O_{4-6}^+$, and $Cr_4O_{7-9}^+$ ions result from the fragmentation of heavier molecules under electron ionization.

Thermodynamic data, previous KEMS studies, and our high power density laser ablation results for CrO_3,; MoO_3, and WO_3 compounds lead us to consider that the formation of the observed stoichiometric $M_nO_{3n}^+$ and part of slightly substoichiometric $M_nO_{3n-2}^+$ and $M_nO_{3n-1}^+$ species results from electron ionization processes of neutral species generated by the laser ablation (i.e., vaporization and sublimation) with electrons produced by the sample laser ablation. Experimental studies involving visible and UV laser ablation of metallic targets have shown that under power density in the 10^8-10^{10} W/cm^2 range, the laser-produced plasma has a typical electron temperature of several electronvolts and a degree of ionization of 1−10% after electron−ion recombination.[8] Moreover, the high laser power density used in our experiment may also lead to neutral multiphotonic absorption in the gas phase. The M_xO_y ionization energy reported in Table 3 and the energy per photon at 193 and 355 nm, 6.42 and 3.49 eV, respectively, may favor thermoionic electron emission in the gas phase. This kind of process has been already reported for other classes of compounds (fullerenes, metal carbides, metal clusters, ...).[59−61] For a $M_xO_y(\in)$ excited neutral cluster, with an internal energy $\in$ of roughly a few tens of electronvolts (absorption of some UV photons), supposed to be randomized over all accessible degrees of freedom, one of the possible desexcitation channel will be eq 6:

$$M_xO_y(\in) \xrightarrow{k_{e^-}} M_xO_y^+ + e^- \quad (6)$$

The energy excess will be converted into kinetic energy.

The highly oxygen-deficient ions are mainly formed by typical aggregation processes. The observation of MoO_3^+ and $Mo_2O_6^+$ ions in the study of molybdenum trioxide at high power density suggests that the kinetic energy of thermal electrons is greater than 16 eV in our instrumental conditions. Indeed, according to Fialko et al.,[33] these ions require a 16 eV kinetic energy in KEMS experiments, in which they are formed by large species fragmentation during electron ionization. According to the appearance potential reported in Table 3, part of the largely

substoichiometric ions may also be formed by electron ionization dissociative processes.

Conclusion

The laser ablation/ionization of CrO_3, MoO_3, and WO_3 compounds at high laser power density leads to the formation of large amounts of $M_xO_y^+$ ions (with M = Cr, Mo, or W). In contrast to other transition-metal oxides, a large fraction of these cluster ions are highly oxygenated. Their formation results from electron ionization processes of neutral species. Neutrals are generated by the heating of the sample at and near the laser impact. Electrons are expelled from the surface according to thermoelectronic and photoelectronic effects. These electrons may gain energy according to IB effect induced by the high laser power density used in our experiment. Alternatively, thermoionic electron emission may occur in the gas phase via M_xO_y neutral multiphotonic absorption processes. When the power density decreases, the temperature reached at the surface decreases. The consequences are, first, the lower emission of thermal electrons and neutral species by vaporization or sublimation or both, second, the decrease of the kinetic energy of the electrons by IB influence decrease, and finally, the decrease of multiphotonic absorption processes. In turn, the production of highly oxygenated ions is less efficient. Only aggregative processes occur and lead to the formation of oxygen-deficient cluster ions. The latter may also be produced, under high power conditions, by ion fragmentation of large molecules during electron impact, according to the high kinetic energy of the electrons.

Even though electrons produced by laser ablation of a metallic target have already been used to ionize organic compounds, to our knowledge, it is the first time that electrons generated by laser ablation of a target induce the ionization of species emitted from its surface. The same kind of process has been recently observed in our group when some polymer compounds were laser ablated. These results will be presented in a separate publication.

References and Notes

(1) Novak, F. P.; Balasanmugan, K.; Viswanadham, K.; Parker, C. D.; Wilk, Z. A.; Mattern, D. *Int. J. Mass Spectrom. Ions Phys.* **1983**, *53*, 135.

(2) Krueger, F. R. *Z. Naturforsch.* **1983**, *38a*, 385.

(3) Schueler, B.; Feigl, P. K. D.; Kruegen, F. R. *Z. Naturforsch.* **1983**, *37a*, 1078.

(4) Jöst, B.; Schueler, B.; Krueger, F. R. *Z. Naturforsch.* **1982**, *37a*, 18.

(5) Miller, J. C., Geohegan, D. B., Eds. *Laser ablation*: *mechanisms and applications II*; AIP Conference Proceedings 288; American Institute of Physics: New York, 1994.

(6) Miller, J. C. *Laser ablation*: *principles and applications*; Springer-Verlag: New York, 1994.

(7) Van Vaeck, L.; Struyf, H.; Van Roy, W.; Adams, F. *Mass Spectrom. Rev.* **1994**, *13*, 189.

(8) Amoruso, S.; Bruzzese, R.; Spinelli, N.; Velotta, R. *J. Phys. B*: *At., Mol. Opt. Phys.* **1999**, *32*, R131.

(9) Marien, J.; DePauw, E. *Anal. Chem.* **1985**, *57*, 362.

(10) Liu, X. H.; Zhang, X. G.; Li, Y.; Wang, X. Y.; Lou, N. Q. *Chem. Phys. Lett.* **1998**, *288*, 804.

(11) Dennemont, J.; Landry, J. C. In *Microbeam Analysis-1985*; Armstrong, J. T., Ed.; San Francisco Press Inc.: San Francisco, CA, 1985; p 305.

(12) Lafargue, P. E.; Gaumet, J. J.; Muller, J. F.; Labrosse, A. *J. Mass Spectrom.* **1996**, *31*, 623.

(13) Gibson, J. K. *J. Appl. Phys.* **1995**, *78*, 1274.

(14) Hachimi, A.; Poitevin, E.; Krier, G.; Muller, J. F.; Ruiz-Lopez, M. F. *Int. J. Mass Spectrom. Ion Processes* **1995**, *144*, 23.

(15) Hachimi, A.; Millon, E.; Poitevin, E.; Muller, J. F. *Analusis* **1993**, *21*, 11.

(16) Liu, X. H.; Zhang, X. G.; Li, Y.; Wang, X. Y.; Lou, N. Q. *Int. J. Mass Spectrom.* **1998**, *177*, L1.

(17) Chaoui, N.; Millon, E.; Muller, J. F. *Chem. Mater.* **1998**, *10*, 3888.

(18) Zhang, X.; Wang, X.; Lou, N. *Prog. Nat. Sci.* **1997**, *7*, 129.

(19) Maunit, B.; Hachimi, A.; Manuelli, P.; Calba, P. J.; Muller, J. F. *Int. J. Mass Spectrom. Ion Processes* **1996**, *156*, 173.

(20) Aubriet, F. Ph.D. Thesis, University of Metz, Metz, France, 1999.

(21) Gibson, J. K. *J. Phys. Chem.* **1994**, *98*, 11321.

(22) Aubriet, F.; Maunit, B.; Muller, J. F. *Int. J. Mass Spectrom.* **2000**, *198*, 213.

(23) Michiels, E.; Gijbels, R. *Anal. Chem.* **1984**, *56*, 1115.

(24) Cassady, C. J.; Weil, D. A.; McElvany, S. W. *J. Chem. Phys.* **1992**, *96*, 691.

(25) Struyf, H.; Van Vaeck, L.; Van Grieken, R. E. *Rapid Commun. Mass Spectrom.* **1996**, *10*, 551.

(26) Van Vaeck, L.; Adriaens, A.; Adams, F. *Spectrochim. Acta* **1998**, *B53*, 367.

(27) Poels, K.; Van Vaeck, L.; Gijbels, R. *Anal. Chem.* **1998**, *70*, 504.

(28) McDonald, J. D.; Margrave, J. L. *J. Inorg. Nucl. Chem.* **1968**, *30*, 665.

(29) Washburn, C. A. Ph.D. Thesis, University of California Berkeley, Berkeley, CA, 1969.

(30) Ling-Fai Wang, J.; Margrave, J. L.; Franklin, J. L. *J. Inorg. Nucl. Chem.* **1975**, *37*, 1107.

(31) Burns, R. P.; DeMaria, G.; Drowart, J.; Grimley, R. T. *J. Chem. Phys.* **1960**, *32*, 1363.

(32) Berkowitz, J.; Inghram, M. G.; Chupka, W. A. *J. Chem. Phys.* **1957**, *26*, 842.

(33) Fialko, E. F.; Kikhtenko, A. V.; Goncharov, V. B.; Zamaraev, K. I. *J. Phys. Chem. A* **1997**, *101*, 8607.

(34) DeMaria, G.; Burns, R. P.; Drowart, J.; Inghram, M. G. *J. Chem. Phys.* **1960**, *32*, 1373.

(35) Ackermann, R. J.; Rauh, E. G. *J. Phys. Chem.* **1963**, *67*, 2596.

(36) Muller, J. F.; Pelletier, M.; Krier, G.; Weil, D.; Campana, J. In *Microbeam Analysis-1989*; Russell, P. E., Ed.; San Francisco Press Inc.: San Francisco, CA, 1989; p 311.

(37) Pelletier, M.; Krier, G.; Muller, J. F.; Weil, D.; Johnston, M. *Rapid Commun. Mass Spectrom.* **1988**, *2*, 146.

(38) Aubriet, F.; Maunit, B.; Courier, B.; Muller, J. F. *Rapid Commun. Mass Spectrom.* **1997**, *11*, 1596.

(39) Cuynen, E.; Van Vaeck, L.; Van Espen, P. *Rapid Commun. Mass Spectrom.* **1999**, *13*, 2287.

(40) Weng, L. T.; Bertrand, P.; Tirions, O.; Devilliers, M. *Appl. Surf. Sci.* **1996**, *99*, 185.

(41) De Smet, F.; Devillers, M.; Poleunis, C.; Bertrand, P. *J. Chem. Soc., Faraday Trans.* **1998**, *94*, 941.

(42) Aubriet, F.; Maunit, B.; Muller, J. F *Int. J. Mass Spectrom.* **2001**, *209*, 5.

(43) Zhou, M.; Andrews, L. *J. Chem. Phys.* **1999**, *111*, 4230.

(44) Wenthold, P. G.; Jonas, K. L.; Lineger, W. C. *J. Chem. Phys.* **1997**, *106*, 9961.

(45) Rudnyi, E. B.; Vovk, O. M.; Kaibicheva, E. A.; Sidorov, L. N. *J. Chem. Thermodyn.* **1989**, *21*, 247.

(46) Maleknia, S.; Brodbelt, J.; Pope, K. *J. Am. Soc. Mass Spectrom.* **1991**, *2*, 212.

(47) Van der Peyl, G. J. Q.; Van der Zande, W. J.; Kistemaker, P. G. *Int. J. Mass Spectrom. Ion Processes* **1984**, *62*, 51.

(48) Vertes, A.; Juhasz, P.; De Wolf, M.; Gijbels, R. *Scanning Microsc.* **1988**, *2*, 1853.

(49) Angotti, M.; Maunît, B.; Muller, J.-F.; Bezdetnaya, L.; Guillemin, F. *J. Mass Spectrom.* **2001**, *36*, 825.

(50) (a) Moritz, F.; Dey, M.; Zipperer, K.; Prinke, S.; Grotemeyer, J. *Org. Mass Spectrom.* **1993**, *28*, 1467. (b) Colby, S. M.; Railly, J. P. *Int. J. Mass Spectrom. Ion Processes* **1994**, *131*, 125. (c) Martinovic, S. Ph.D. Thesis, University of Metz, Metz, France, 1997.

(51) *CRC Handbook of Chemistry and Physics*, 73rd ed.; Lide, D. R., Ed.; CRC: Boca Raton, FL, 1992−1993.

(52) Mao, S. S.; Mao, X. L.; Greil, R.; Russo, R. E. *Appl. Surf. Sci.* **1998**, *127*−*129*, 206.

(53) Eloy, J.-F. *Les lasers de puissance, applications*; Masson: Paris, 1985.

(54) Boulmer-Leborgne, C; Hermann, J.; Dubreuil, B. *Plasma Sources Sci. Technol.* **1993**, *2*, 219.

(55) Fiedler, A.; Kretzhmar, I.; Schöder, D.; Schwarz, H. *J. Am. Chem. Soc.* **1996**, *118*, 9941.

(56) Grimley, R. T.; Burns, R. P.; Inghram, M. G. *J. Chem. Phys.* **1961**, *34*, 664.

(57) Benett, S. L.; Liu, S. S.; Gilles, P. W. *J. Phys. Chem.* **1974**, *78*, 266.

(58) Norman, J. H.; Staley, H. G. *J. Chem. Phys.* **1965**, *43*, 3804.

(59) Anderson, J. U.; Bontemps, E.; Hansen, K. *J. Phys. B* **2002**, *35*, R1.

(60) Van Heijnsbergen, D.; Von Helden, G.; Duncan, M. A.; Van Roij, A. J. A.; Meijer, G. *Phys. Rev. Lett.* **1999**, *83*, 4983.

(61) Deng, R.; Echt, O. *J. Phys. Chem. A* **1998**, *102*, 2533.